NASA/TM–2019–220429

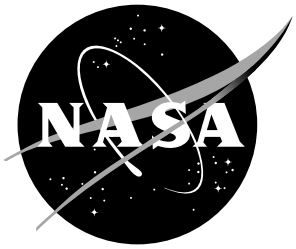

An Initial Exploration of Improved Numerics within the Guidelines of the Negative Spalart-Allmaras Turbulence Model

William K. Anderson,[1] *Stephen L. Wood,*[1] *Steven R. Allmaras*[2]

1: Langley Research Center, Hampton, Virginia
2: Massachusetts Institute of Technology, Boston, Massachusetts

November 2019

NASA STI Program. . . in Profile

Since its founding, NASA has been dedicated to the advancement of aeronautics and space science. The NASA scientific and technical information (STI) program plays a key part in helping NASA maintain this important role.

The NASA STI Program operates under the auspices of the Agency Chief Information Officer. It collects, organizes, provides for archiving, and disseminates NASA's STI. The NASA STI Program provides access to the NASA Aeronautics and Space Database and its public interface, the NASA Technical Report Server, thus providing one of the largest collection of aeronautical and space science STI in the world. Results are published in both non-NASA channels and by NASA in the NASA STI Report Series, which includes the following report types:

- TECHNICAL PUBLICATION. Reports of completed research or a major significant phase of research that present the results of NASA programs and include extensive data or theoretical analysis. Includes compilations of significant scientific and technical data and information deemed to be of continuing reference value. NASA counterpart of peer-reviewed formal professional papers, but having less stringent limitations on manuscript length and extent of graphic presentations.
- TECHNICAL MEMORANDUM. Scientific and technical findings that are preliminary or of specialized interest, e.g., quick release reports, working papers, and bibliographies that contain minimal annotation. Does not contain extensive analysis.
- CONTRACTOR REPORT. Scientific and technical findings by NASA-sponsored contractors and grantees.
- CONFERENCE PUBLICATION. Collected papers from scientific and technical conferences, symposia, seminars, or other meetings sponsored or co-sponsored by NASA.
- SPECIAL PUBLICATION. Scientific, technical, or historical information from NASA programs, projects, and missions, often concerned with subjects having substantial public interest.
- TECHNICAL TRANSLATION. English-language translations of foreign scientific and technical material pertinent to NASA's mission.

Specialized services also include organizing and publishing research results, distributing specialized research announcements and feeds, providing information desk and personal search support, and enabling data exchange services.

For more information about the NASA STI Program, see the following:

- Access the NASA STI program home page at `http://www.sti.nasa.gov`
- E-mail your question to `help@sti.nasa.gov`
- Phone the NASA STI Information Desk at 757-864-9658
- Write to:
  NASA STI Information Desk
  Mail Stop 148
  NASA Langley Research Center
  Hampton, VA 23681-2199

NASA/TM–2019–220429

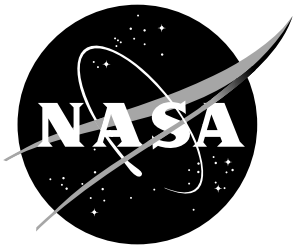

An Initial Exploration of Improved Numerics within the Guidelines of the Negative Spalart-Allmaras Turbulence Model

William K. Anderson,[1] *Stephen L. Wood,*[1] *Steven R. Allmaras*[2]

1: Langley Research Center, Hampton, Virginia
2: Massachusetts Institute of Technology, Boston, Massachusetts

National Aeronautics and
Space Administration

Langley Research Center
Hampton, Virginia 23681-2199

November 2019

Available from:

NASA STI Program / Mail Stop 148
NASA Langley Research Center
Hampton, VA 23681-2199
Fax: 757-864-6500

Abstract

A simple modification to the negative Spalart-Allmaras turbulence model is suggested so that when the turbulence working variable, $\widetilde{\nu}$, is negative, diagonal dominance is increased, as is the tendency for the time-advancement scheme to push $\widetilde{\nu}$ toward positive values. Owing to the fact that the modification is only active when $\widetilde{\nu}$ is less than zero, the physical model is left unchanged. Using the proposed modification with a strong implicit solver based on Newton's method, convergence rates can be somewhat improved, with typical reductions in iterations and computer time on the order of $15 - 50\%$. The benefits are realized primarily when second- or higher-order accuracy is used for discretizing the convective terms in the turbulence model because of large overshoots that can occur with these schemes at the edges of boundary layers and wakes. For flowfields with few regions of negative $\widetilde{\nu}$, or on very fine meshes where $\widetilde{\nu}$ is always greater than zero, little or no benefits should be expected.

1 Introduction

The negative Spalart-Allmaras (SA-neg) turbulence model, as introduced by Allmaras et al. [1], allows for continuous time integration of the turbulence model when the working variable, $\widetilde{\nu}$, is negative. Although, in principle, negative values of $\widetilde{\nu}$ only occur because of insufficient mesh resolution, simulations on practical meshes in routine use for engineering computations inevitably contain negative values at the edges of boundary layers and wakes. With second-, and higher-, order discretization of the turbulence model, these values may reach magnitudes as large as several thousand that of the kinematic viscosity. For these regions, reference [1] provides general requirements, and initial suggestions, for discretizing the production, destruction, and diffusion terms so that the turbulence working variable effectively becomes a passive scalar, thereby allowing integration to continue without having concern for generating negative eddy viscosity. However, while the initial suggestions are quite effective, considerable latitude exists for alternate discretizations that also fit within the guidelines, but which may provide numerical benefits.

In this paper, an inceptive modification is suggested for the destruction term when $\widetilde{\nu}$ is less than zero. This simple modification increases the tendency to drive $\widetilde{\nu}$ toward positive values and also increases diagonal dominance. These features particularly benefit implicit solvers based on Newton's method that solve the flow equations and the turbulence model tightly coupled, and use strong linear solvers and preconditioners. For these solvers, increasing diagonal dominance can be quite beneficial to both robustness and speed of convergence.

2 Governing Equations

The governing equations are the compressible, Reynolds-averaged Navier-Stokes equations augmented with the one-equation SA-neg turbulence model [1]. The equations can be expressed in the following conservative form:

$$\frac{\partial \mathbf{Q}(\mathbf{x},t)}{\partial t} + \nabla \cdot (\mathbf{F}_e(\mathbf{Q}) - \mathbf{F}_v(\mathbf{Q},\nabla\mathbf{Q})) = \mathbf{S}(\mathbf{Q},\nabla\mathbf{Q}) \quad \text{in} \quad \Omega \tag{1}$$

where Ω is a bounded domain. The vector of conservative flow variables $\mathbf{Q}$, the inviscid and viscous Cartesian flux vectors, $\mathbf{F}_e$ and $\mathbf{F}_v$, are defined by:

$$\mathbf{Q} = \begin{bmatrix} \rho \\ \rho u \\ \rho v \\ \rho w \\ \rho E \\ \rho\tilde{\nu} \end{bmatrix}, \quad \mathbf{F}_e^x = \begin{bmatrix} \rho u \\ \rho u^2 + p \\ \rho uv \\ \rho uw \\ (\rho E + p)u \\ \rho u\tilde{\nu} \end{bmatrix}, \quad \mathbf{F}_e^y = \begin{bmatrix} \rho v \\ \rho uv \\ \rho v^2 + p \\ \rho vw \\ (\rho E + p)v \\ \rho v\tilde{\nu} \end{bmatrix}, \quad \mathbf{F}_e^z = \begin{bmatrix} \rho w \\ \rho uw \\ \rho vw \\ \rho w^2 + p \\ (\rho E + p)w \\ \rho w\tilde{\nu} \end{bmatrix} \tag{2}$$

$$\mathbf{F}_v^x = \begin{bmatrix} 0 \\ \tau_{xx} \\ \tau_{xy} \\ \tau_{xz} \\ u\tau_{xx} + v\tau_{xy} + w\tau_{xz} + \kappa\frac{\partial T}{\partial x} \\ \frac{1}{\sigma}\rho(\nu + \tilde{\nu}f_n)\frac{\partial \tilde{\nu}}{\partial x} \end{bmatrix}, \quad \mathbf{F}_v^y = \begin{bmatrix} 0 \\ \tau_{xy} \\ \tau_{yy} \\ \tau_{yz} \\ u\tau_{xy} + v\tau_{yy} + w\tau_{yz} + \kappa\frac{\partial T}{\partial y} \\ \frac{1}{\sigma}\rho(\nu + \tilde{\nu}f_n)\frac{\partial \tilde{\nu}}{\partial y} \end{bmatrix},$$

$$\mathbf{F}_v^z = \begin{bmatrix} 0 \\ \tau_{xz} \\ \tau_{yz} \\ \tau_{zz} \\ u\tau_{xz} + v\tau_{yz} + w\tau_{zz} + \kappa\frac{\partial T}{\partial z} \\ \frac{1}{\sigma}\rho(\nu + \tilde{\nu}f_n)\frac{\partial \tilde{\nu}}{\partial z} \end{bmatrix}. \tag{3}$$

Here, ρ , p, and E denote the fluid density, pressure, and total energy per unit mass, respectively, $\mathbf{u} = (u, v, w)$ represents the Cartesian velocity vector, and $\tilde{\nu}$ represents the turbulence working variable in the negative SA model. The pressure p is determined by the equation of state for an ideal gas,

$$p = (\gamma - 1)\left(\rho E - \frac{1}{2}\rho(u^2 + v^2 + w^2)\right) \tag{4}$$

where γ is the ratio of specific heats, which is 1.4 for air. The subscripts on τ represent the components of the viscous stress tensor, which is defined for a Newtonian fluid as,

$$\tau_{ij} = (\mu + \mu_T)\left(\frac{\partial \mathbf{u}_i}{\partial \mathbf{x}_j} + \frac{\partial \mathbf{u}_j}{\partial \mathbf{x}_i} - \frac{2}{3}\frac{\partial \mathbf{u}_k}{\partial \mathbf{x}_k}\delta_{ij}\right) \tag{5}$$

where δ_{ij} is the Kronecker delta and subscripts i, j, k refer to the Cartesian coordinate components for $\mathbf{x} = (x, y, z)$. μ refers to the fluid dynamic viscosity and is obtained via Sutherland's law [2]. In Eq. 5, μ_T denotes the turbulence eddy viscosity, which is obtained from the negative SA model by:

$$\mu_T = \begin{cases} \rho\tilde{\nu}f_{v1} & \text{if } \tilde{\nu} \geq 0 \\ 0 & \text{if } \tilde{\nu} < 0 \end{cases} \tag{6}$$

The source term, $\mathbf{S}$, in Eq. 1 is given by $\mathbf{S} = [0, 0, 0, 0, 0, S_t]^T$, where the components for the continuity, momentum and energy equations are zero. The source term corresponding to the turbulence model equation takes the following form [1]:

$$S_t = P - D + \frac{1}{\sigma}c_{b2}\rho\nabla\tilde{\nu}\cdot\nabla\tilde{\nu} - \frac{1}{\sigma}(\nu + \tilde{\nu}f_n)\nabla\rho\cdot\nabla\tilde{\nu} \tag{7}$$

where the production term is given as

$$P = \begin{cases} c_{b1}\rho(1-f_{t2})\tilde{S}\tilde{\nu} & \text{if } \tilde{\nu} \geq 0 \\ c_{b1}\rho(1-c_{t3})S\tilde{\nu} & \text{if } \tilde{\nu} < 0 \end{cases} \tag{8}$$

and the destruction term is defined as

$$D = \begin{cases} \rho(c_{w1}f_w - \frac{c_{b1}}{\kappa_t^2}f_{t2})(\frac{\tilde{\nu}}{d})^2 & \text{if } \tilde{\nu} \geq 0 \\ -\rho c_{w_1}(\frac{\tilde{\nu}}{d})^2 & \text{if } \tilde{\nu} < 0. \end{cases} \tag{9}$$

In Eq. 7, 8, and 9, ν denotes kinematic viscosity that is the ratio of dynamic viscosity to density, μ/ρ. Additional definitions associated with the production and destruction terms are given as [1]:

$$\tilde{S} = \begin{cases} S + \hat{S} & \text{if } \hat{S} \geq -c_{v2}S \\ S + \frac{S(c_{v2}^2 + c_{v3}\hat{S})}{(c_{v3}-2c_{v2})S - \hat{S}} & \text{if } \hat{S} < -c_{v2}S \end{cases} \tag{10}$$

$$S = \sqrt{\vec{\omega}\cdot\vec{\omega}}, \quad \hat{S} = \frac{\tilde{\nu}}{\kappa_t^2 d^2}f_{v2}, \quad f_{v1} = \frac{\chi^3}{\chi^3 + c_{v1}^3}, \tag{11}$$

$$f_{v2} = 1 - \frac{\chi}{1+\chi f_{v1}}, \quad f_{t2} = c_{t3}e^{-c_{t4}\chi^2} \tag{12}$$

and

$$\chi = \frac{\tilde{\nu}}{\nu}, \quad r = \min(\frac{\tilde{\nu}}{\tilde{S}\kappa_t^2 d^2}r_{\lim}), \quad g = r + c_{w2}(r^6 - r), \quad f_w = g\left(\frac{1+c_{w3}^6}{g^6 + c_{w3}^6}\right)^{1/6} \tag{13}$$

where the vorticity vector is given by, $\vec{\omega} = \nabla \times \mathbf{u}$ and d represents the distance to the nearest wall.

The constants in the negative SA model are given as: $c_{b1} = 0.1355$, $\sigma = 2/3$, $c_{b2} = 0.622$, $c_{t3} = 1.2$, $c_{t4} = 0.5$, $\kappa_t = 0.41$, $c_{w1} = c_{b1}/\kappa_t^2 + (1 + c_{b2})/\sigma$, $c_{w2} = 0.3$, $c_{w3} = 2$ $c_{v1} = 7.1$, $c_{v2} = 0.7$ and $c_{v3} = 0.9$. κ and T denote the thermal conductivity and temperature, respectively, and are related to the total energy and velocity as,

$$\kappa T = \gamma(\frac{\mu}{P_r} + \frac{\mu_T}{P_{r_T}})\left(E - \frac{1}{2}(u^2 + v^2 + w^2)\right) \tag{14}$$

where P_r and P_{r_T} are the Prandtl and turbulent Prandtl number that are set to 0.72 and 0.9, respectively. In the case of laminar flow, the governing equations reduce to the compressible Navier-Stokes equations, where the turbulence model equation is deactivated and the turbulence eddy viscosity, μ_T, in the fluid viscous stress tensor and the thermal conduction term vanishes.

For the purpose of the spatial discretization, the Cartesian viscous fluxes are rewritten in the following equivalent form:

$$\mathbf{F}_v^x = \mathbf{G}_{1j}\frac{\partial \mathbf{Q}}{\partial \mathbf{x}_j}, \quad \mathbf{F}_v^y = \mathbf{G}_{2j}\frac{\partial \mathbf{Q}}{\partial \mathbf{x}_j}, \quad \mathbf{F}_v^z = \mathbf{G}_{3j}\frac{\partial \mathbf{Q}}{\partial \mathbf{x}_j} \tag{15}$$

where the matrices $\mathbf{G}_{ij}(\mathbf{Q})$ are determined by $\mathbf{G}_{ij} = \partial \mathbf{F}_v^{x_i}/\partial(\partial \mathbf{Q}/\partial \mathbf{x}_j)$ for $i, j = 1, 2, 3$.

3 Spatial Discretization

For the current work, a continuous Galerkin finite-element method is used, where the domain of interest is discretized into a series of nonoverlapping elements, and the field variables are assumed continuous across element boundaries. Single-valued data are stored at the vertices of the elements and the solution is assumed to vary within each element according to a linear combination of polynomial basis functions

$$\mathbf{Q}_h = \sum_{i=1}^{n} N_i \mathbf{Q}_i \tag{16}$$

Here, $\mathbf{Q}_h$ represents the dependent variables approximated within each element, $\mathbf{Q}_i$ are the corresponding data at the nodes of the element, and each N_i represents a basis function.

The spatial discretization is a Streamlined-Upwind Petrov-Galerkin (SUPG) finite-element method described in Ref. [3]. The SUPG finite-element scheme is formulated as a weighted residual method, which can be cast in the form shown below

$$\int_\Omega (N_i + P_i)\left(\frac{\partial \mathbf{Q}}{\partial t} + \nabla \cdot \mathbf{F} - \mathbf{S}\right) d\Omega = 0 \tag{17}$$

where P_i, is a stabilizing term that provides dissipation along preferential directions to eliminate odd-even point decoupling that often occurs with the standard Galerkin scheme that is obtained if P_i is neglected. In the present work, the Streamlined Upwind Petrov-Galerkin (SUPG) method is used in defining the weighting function [4].

$$P_i = \left(\frac{\partial N}{\partial x}[A] + \frac{\partial N}{\partial y}[B] + \frac{\partial N}{\partial z}[C]\right)[\tau] \tag{18}$$

$$[\tau]^{-1} = \sum_{j=1}^{M}\left(\left|\frac{\partial N_j}{\partial x_i}[\mathbf{A}_i]\right| + \frac{\partial N_j}{\partial x_i}[\mathbf{G}_{ik}]\frac{\partial N_j}{\partial x_k}\right) \tag{19}$$

$$\left|\frac{\partial N_j}{\partial x_i}[\mathbf{A}_i]\right| = [\mathbf{T}]\,|\Lambda|\,[\mathbf{T}]^{-1}. \tag{20}$$

Here, M corresponds to the number of basis functions within the element and the repeated index, i,j, and k imply summation over all the values ($i, j, k = 1, 2, 3$), and the definitions of $[\mathbf{G}_{ik}]$ corresponds to those given in Eq. 15.

The matrices $[\Lambda]$ and $[T]$ are the eigenvalues and right eigenvectors, respectively, of the matrix on the left side of Eq. 20 whereas the inverse of $[T]$ is given by $[T]^{-1}$. The resulting weak statement may be written as

$$\int_\Omega (N\frac{\partial \mathbf{Q}}{\partial t} - \nabla N \cdot \mathbf{F} \cdot - N\mathbf{S}) d\Omega + \int_\Omega [P] \left\{ \frac{\partial \mathbf{Q}}{\partial t} + \nabla \cdot \mathbf{F} - \mathbf{S} \right\} d\Omega + \int_\Gamma N\mathbf{F} \cdot n d\Gamma = 0 \tag{21}$$

In evaluating the volume and surface integrals, Gaussian quadrature rules are used where, for polynomial representations of the dependent variables of order p, the volume integrals are evaluated using formulas appropriate for integrating polynomials of order 2p whereas surface integrals are integrated using formulas for integrating polynomials of order 2p + 1 [6]. Note that because the field variables are assumed to be continuous in the interior of the domain, the surface integral typically vanishes on the boundaries of the interior elements and need only be evaluated on the boundaries of the domain where appropriate boundary conditions are applied as discussed in Ref. [3].

4 Time Advancement

To advance the solution toward a steady state, the density, velocity components, temperature, and the turbulence-model working variable are tightly coupled and updated using a Newton-type algorithm described in Ref. [3].

Here, an initial update to the flow variables is computed using a locally varying time-step parameter that is multiplied by the current CFL number, which is adjusted during the iterative process to provide global convergence. Using the full update of the variables, the L_2 norm of the unsteady residual is compared to its value at the beginning of the iteration. If the L_2 norm after the update is less than a prespecified target value relative to the original value, the the CFL number is increased by a multiplicative factor, typically 1.25. If the L_2 norm reduction target is not met, a line search is conducted to determine an appropriate relaxation factor and the CFL number is neither increased nor decreased.

In contrast to the methodology described in Ref. [3], if slow convergence of the linear system at any step is detected, the entire step is rejected and the CFL number is lowered. Here, the determination is made simply by requiring

the residual of the linear system to be reduced by a factor of two. Rejecting steps when the linear system is not reduced by this minimal step reduces the frequency of accepting updates that do not help reduce the residual of the nonlinear system. As a result, the nonlinear iterative process is more robust.

5 Modification of the Destruction Term

The purpose of developing the SA negative turbulence model was to provide a continuation of the original SA model so that negative values of $\widetilde{\nu}$, that occur at undershoots and during nonphysical transients, do not force the simulation to halt [1]. In developing the model, five guidelines were originally provided [1]:

- The original SA model is unchanged when $\widetilde{\nu} \geq 0$
- Negative values of $\widetilde{\nu}$ produce zero eddy viscosity
- Functions in the partial differential equation are C^1 continuous with respect to $\widetilde{\nu}$ at $\widetilde{\nu} = 0$
- Negative SA is energy stable
- The analytic solution is nonnegative given nonnegative boundary conditions

To achieve these objectives, the diffusion, production, and wall destruction terms have been defined as given above in Eqs. 7, 8, and 9, respectively. However, simple modifications, in particular to the destruction term, can be made to enhance the numerical behavior when $\widetilde{\nu}$ is negative. Specifically, note that when $\widetilde{\nu}$ is negative, the sign of the destruction term is such that this term essentially becomes a production term tending to drive the turbulence working variable positive. Secondly, the linearization of the destruction term adds to the diagonal a term proportional to $-\rho c_{w1}\widetilde{\nu}/d^2$. Because $\widetilde{\nu}$ is negative, the term added to the diagonal is positive, thereby increasing diagonal dominance. Both effects are beneficial to the numerical integration of the turbulence model. As such, one could expect numerical benefits by simply multiplying the destruction term by a constant, α, to "boost" the destruction term as indicated in Eq. 22.

$$D = \begin{cases} \rho(c_{w1}f_w - \frac{c_{b1}}{\kappa_t^2}f_{t2})(\frac{\tilde{\nu}}{d})^2 & \text{if } \tilde{\nu} \geq 0 \\ -\alpha\rho c_{w_1}(\frac{\tilde{\nu}}{d})^2 & \text{if } \tilde{\nu} < 0. \end{cases} \tag{22}$$

Note that the benefits discussed above are realized for $\alpha > 1.0$. However, increasing α also increases the nonlinearity of the scheme so that one might expect practical limits to the magnitude, beyond which benefits might be negated. In practice, the value of α is typically set to 10, although numerical tests indicate similar results over a range of values as high as 50, so that the precise value is not critical.

Although not presented here, replacing the form of the destruction term with a more general curve that blends smoothly from a quadratic when $\widetilde{\nu}$ is near zero, into a linear function for large negative values of $\widetilde{\nu}$, have also been explored. The objective in these experiments is to decrease nonlinearity as $\widetilde{\nu}$ gets larger in magnitude. However, experiments to date indicate that good results are obtained by simply multiplying by a constant, without regard to decreasing nonlinearity. However, further explorations are planned.

6 Results

For strong solvers based on Newton's method, increasing diagonal dominance can be quite beneficial to robustness and for increasing the rate of convergence. Two example simulations are provided below. In each case, solutions obtained using the negative SA model as described in Ref. [1] are labeled as having a "boosting" parameter of 1.0, whereas the results with a boosting coefficient of 10.0 are labelled appropriately.

The first example demonstrates the benefits of the proposed modification using the finite-element solver described above. The configuration corresponds to that of Case 2a from the AIAA 3rd High-Lift Prediction Workshop [7], which is a high-lift geometry at a freestream Mach number of 0.172, a Reynolds number of 1.93×10^6 based on the mean aerodynamic chord, and an angle of attack of 10.47°. The mesh used for the simulation has been obtained using the adaptive methodology described in Ref. [8], with the geometry and mesh both depicted in Fig.1(a). As seen in the figure, the simulation includes the nacelles, flaps, and slats for the configuration under consideration. The mesh, resulting after ten adaptation cycles, is comprised of $8,988,908$ nodes, $47,920,723$ tetrahedrons, with $1,778,232$ triangular elements on the surface. The mesh is very highly anisotropic and provides high resolution of the complex wake structure behind the vehicle.

The convergence histories for this case are shown in Fig. 1(b), where 320 cores have been used for the simulation. As seen, solutions are obtained to machine accuracy whether or not boosting is used. Note that the residual for the turbulence model is somewhat lower than for the flow equations, which are nominally at machine precision. This is because the turbulence working variable is linearly scaled at the beginning of the iterative process as described in Ref. [3] to prevent the turbulence model from dominating the behavior of the CFL controller. However, using a boosting coefficient of 10.0, convergence is reached in almost 200 fewer iterations than without boosting. Although not shown, a similar savings in computer time, of approximately 30% is realized.

The magnitude of the turbulence working variable is shown in Fig. 2. Here, Fig. 2(a) depicts $\widetilde{\nu}/\nu_\infty$, as well as the mesh, extending from slightly ahead of the geometry to a plane located 65 chord lengths downstream. A closeup of

$\widetilde{\nu}/\nu_\infty$ on the backplane is seen in Fig. 2(b), where the maximum value in the center of the vortex is approximately $45,000$. To highlight the presence of overshoots, and large negative values, Fig. 2(c) shows $\widetilde{\nu}/\nu_\infty$ restricted to only negative values. Note that a different colormap has been used to facilitate easily visualizing the values. In this figure, the light yellow/red on the back plane represent values of $\widetilde{\nu}/\nu_\infty$ about -520. Moving only one cell away from a yellow contour, toward the vortex center, the corresponding value of $\widetilde{\nu}/\nu_\infty$ is over 1200. Similarly, on the symmetry plane, the red contours near the vortex have values of $\widetilde{\nu}/\nu_\infty$ near -1800. Furthermore, on the symmetry plane, alternating yellow/gray contours are observed. These regions are indicative of oscillations in the turbulence working variable ranging between -1400 up to 300 over just a few cells. These oscillations in the turbulence working variable indicate that the turbulence model solution is not properly resolved [1]. Clearly, overshoots in the wake area are prevalent in this flowfield, so that benefits of boosting the destruction term are expected.

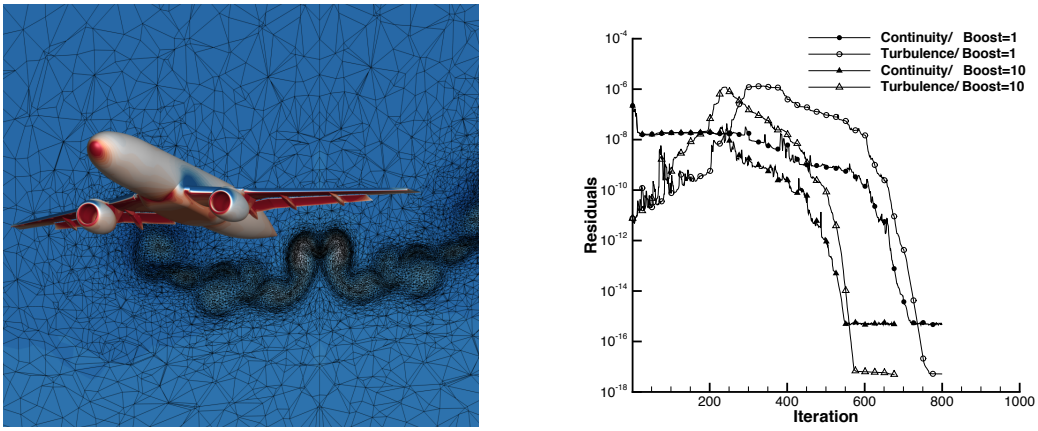

(a) Geometry and mesh.

(b) Convergence history.

Figure 1. Geometry, mesh, and convergence history for high-lift test case.

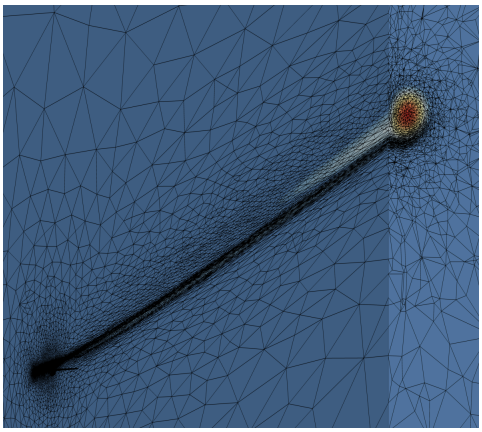

(a) Farfield view..

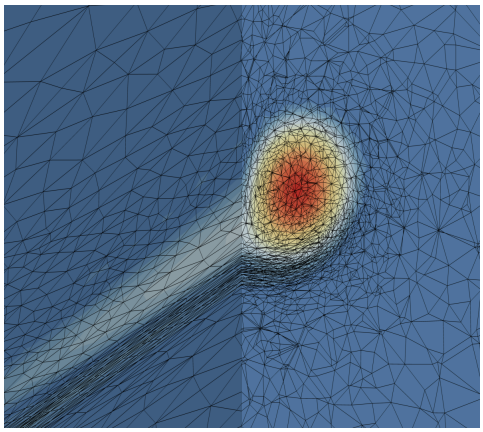

(b) $\widetilde{\nu}$ near backplane.

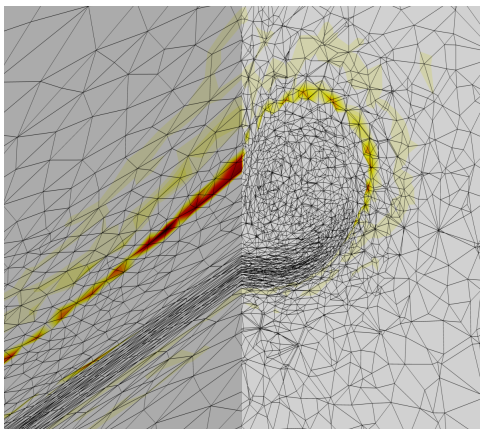

(c) Negative values of $\widetilde{\nu}$ near backplane.

Figure 2. Turbulence working variable for high-lift test case.

For independent confirmation of the benefits that may be achievable using boosting, the COFFE [9] finite-element solver has been used. For this result, the geometry is the Common Research Model (CRM) used during the AIAA 4th Drag Prediction Workshop [10]. This geometry is a cruise-type of geometry at a freestream Mach number is 0.85, a Reynolds number of 5×10^6 based on the mean aerodynamic chord, and angle of attack is 2.33°. The simulation was performed on 528 cores, using a mesh consisting of $17,891,069$ nodes and $106,012,944$ tetrahedrons. Table 1 shows the number of iterations, as well as the wall-clock time to converge the solutions. As with the high-lift case above, boosting the destruction term when $\widetilde{\nu}$ is less than zero provides substantial benefits in terms of reducing the cost of the computation. In this example, the number of iterations has been cut by over a factor of 3, and the wall-clock time is reduced by half.

Table 1. Convergence for DPW4 configuration with/without boosting.

α	Iterations	Wall-clock time
1.0	840	19h 16m
10.0	232	8h 29m

7 Summary and Discussion

A very simple modification to the SA-neg turbulence model, requiring only changing a single line of source code, has been proposed and the benefits to convergence have been verified using two different solvers. It should be noted, however, that the two solvers have several similarities in that they both solve the flow equations and turbulence model tightly coupled, both use SUPG finite-element discretizations, and both use Newton-type algorithms with strong linear solvers to advance the solution at each time step. Nevertheless, increasing diagonal dominance is normally advantageous for robustness and convergence of iterative processes. The results included here also demonstrate that while the initial suggestions in Ref. [1] for discretization of the production, destruction, and diffusion terms provide a robust algorithm for simulating very complex flows with the SA turbulence model, other possibilities are within the suggested guidelines that may provide further benefit. While only one simple modification has been demonstrated in this report, work will undoubtedly continue to make further improvements.

8 Acknowledgments

This research was sponsored by the NASA Transformational Tools and Technologies (TTT) Project of the Transformative Aeronautics Concepts Program under the Aeronautics Research Mission Directorate.

The authors also acknowledge and thank Ryan Glasby for performing an independent study of the modification proposed in this work and sharing results.

References

1. Allmaras, S. R.; Johnson, F. T.; and Spalart, P. R.: Modifications and Clarifications for the Implementation of the Spalart-Allmaras Turbulence Model. *Seventh International Conference on Computational Fluid Dynamics (ICCFD7)*, 2012.

2. White, F. M.; and Corfield, I.: *Viscous fluid flow*, vol. 3. McGraw-Hill New York, 2006.

3. Anderson, W. K.; Newman, J. C.; and Karman, S. L.: Stabilized Finite Elements in FUN3D. *Journal of Aircraft*, vol. 55, no. 2, 2018, pp. 696–714.

4. Bonhaus, D. L.: A Higher Order Accurate Finite Element Method for Viscous Compressible Flows. Ph.D. Thesis, Virginia Polytechnic Institute and State University, 1998.

5. Barth, T. J.: Numerical Methods for Gasdynamic Systems on Unstructured Grids. *An Introduction to Recent Developments in Theory and Numerics for Conservation Laws*, D. Kroner, M. Ohlberger, and C. Rohde, eds., Lecture Notes in Computational Science and Engineering, Springer, 1998, pp. 195–285.

6. Cockburn, B.; Hou, S.; and Shu, C.-W.: The Runge-Kutta local projection discontinuous Galerkin finite element method for conservation laws. IV. The multidimensional case. *Mathematics of Computation*, vol. 54, no. 190, 1990, pp. 545–581.

7. Rumsey, C. L.; Slotnick, J. P.; and Sclafani, A. J.: *Overview and Summary of the Third AIAA High Lift Prediction Workshop*. URL https://arc.aiaa.org/doi/abs/10.2514/6.2018-1258.

8. Balan, A.; Park, M. A.; and Anderson, W. K.: *Adjoint-based Anisotropic Mesh Adaptation for a Stabilized Finite-Element Flow Solver*. URL https://arc.aiaa.org/doi/abs/10.2514/6.2019-2949.

9. Glasby, R.; Erwin, T.; Stefanski, D. L.; Allmaras, S.; Galbraith, M. C.; Anderson, W. K.; and Nichols, R. H.: Introduction to COFFE: The Next-Generation HPCMP CREATE-AV CFD Solver. AIAA Paper 2016–0567, 2016.

10. Vassberg, J. C.; DeHaan, M. A.; Rivers, M. S.; and Wahls, R. A.: Retrospective on the Common Research Model for Computational Fluid Dynamics Validation Studies. *Journal of Aircraft*, vol. 55, no. 4, 2018, pp. 1325–1337. URL https://doi.org/10.2514/1.C034906.

REPORT DOCUMENTATION PAGE

Form Approved
OMB No. 0704–0188

1. REPORT DATE *(DD-MM-YYYY)*	2. REPORT TYPE	3. DATES COVERED *(From - To)*
01-11-2019	Technical Memorandum	

4. TITLE AND SUBTITLE
An Initial Exploration of Improved Numerics within the Guidelines of the Negative Spalart-Allmaras Turbulence Model

5a. CONTRACT NUMBER

5b. GRANT NUMBER

5c. PROGRAM ELEMENT NUMBER

6. AUTHOR(S)
Anderson, William K.;[1] Wood, Stephen L.[1] Allmaras, Steven R.[2]

5d. PROJECT NUMBER

5e. TASK NUMBER

5f. WORK UNIT NUMBER
109492.02.07.01.01.01

7. PERFORMING ORGANIZATION NAME(S) AND ADDRESS(ES)
NASA Langley Research Center
Hampton, Virginia 23681-2199

8. PERFORMING ORGANIZATION REPORT NUMBER
L–21086

9. SPONSORING/MONITORING AGENCY NAME(S) AND ADDRESS(ES)
National Aeronautics and Space Administration
Washington, DC 20546-0001

10. SPONSOR/MONITOR'S ACRONYM(S)
NASA

11. SPONSOR/MONITOR'S REPORT NUMBER(S)
NASA/TM–2019–220429

12. DISTRIBUTION/AVAILABILITY STATEMENT
Unclassified-Unlimited
Subject Category 64
Availability: NASA STI Program (757) 864-9658

13. SUPPLEMENTARY NOTES
An electronic version can be found at http://ntrs.nasa.gov.

14. ABSTRACT

A simple modification to the negative Spalart-Allmaras turbulence model is suggested so that when the turbulence working variable, $\widetilde{\nu}$, is negative, diagonal dominance is increased, as is the tendency for the time-advancement scheme to push $\widetilde{\nu}$ toward positive values. Owing to the fact that the modification is only active when $\widetilde{\nu}$ is less than zero, the physical model is left unchanged. Using the proposed modification with a strong implicit solver based on Newton's method, convergence rates can be somewhat improved, with typical reductions in iterations and computer time on the order of $15 - 50\%$. The benefits are realized primarily when second- or higher-order accuracy is used for discretizing the convective terms in the turbulence model because of large overshoots that can occur with these schemes at the edges of boundary layers and wakes. For flowfields with few regions of negative $\widetilde{\nu}$, or on very fine meshes where $\widetilde{\nu}$ is always greater than zero, little or no benefits should be expected.

15. SUBJECT TERMS
Numerical Analysis; Computational fluid dynamics; Mathematics

16. SECURITY CLASSIFICATION OF:			17. LIMITATION OF ABSTRACT	18. NUMBER OF PAGES	19a. NAME OF RESPONSIBLE PERSON
a. REPORT	b. ABSTRACT	c. THIS PAGE			STI Information Desk (help@sti.nasa.gov)
U	U	U	UU	19	19b. TELEPHONE NUMBER *(Include area code)* (757) 864-9658